Chapter 6

6.1 Introduction

This chapter investigates the evolution of structure and resistive switching behavior in pristine and Sm, Dy doped HfO_2 thin films. The grazing incidence X-ray diffraction (GIXRD) reveals that while pristine film exhibits the monoclinic phase of HfO_2, the high temperature cubic phase is stabilized at room temperature in Sm and Dy doped HfO_2 films after doping almost half of the concentration compared to 12 at% of Sm or 11 at% of Dy in HfO_2nanoparticles reported by us.[189, 190] The fabricated HfO_2 based RRAM devices exhibit the bipolar forming-free resistive switching behavior. The role of oxygen vacancy formation in the stabilization of cubic phase as well as the resistive switching behavior in Sm and Dy doped HfO_2films are discussed.

6.2 Results and Discussion

6.2.1 X-ray Reflectivity and Phase transformation

Figure 6.1 (a-c) depict XRR data of HfO_2, Sm:HfO_2 and Dy:HfO_2, respectively. In order to evaluate the film density and thickness, XRR data have been fitted with suitable stack models using Parratt software. In XRR pattern, the thickness and density are estimated from the critical angle for external reflection and period of the oscillations, respectively. The fittings show that the observed data and simulated curves are in good agreement in case of all thin films. For HfO_2, Sm:HfO_2 and Dy:HfO_2 films, the thickness is estimated as ~59.8, 59 and 58 nm, respectively. The film density is found to be 9.2, 8.4 and 8.1 g/cm^3 corresponding to HfO_2, Sm:HfO_2 and Dy:HfO_2 films, respectively. In addition,

from EDS spectra, the atomic concentrations of Sm and Dy ions are found to be ~5.56 and ~4.46 at% in Sm and Dy doped HfO_2 films, respectively (**figure 6.2**).

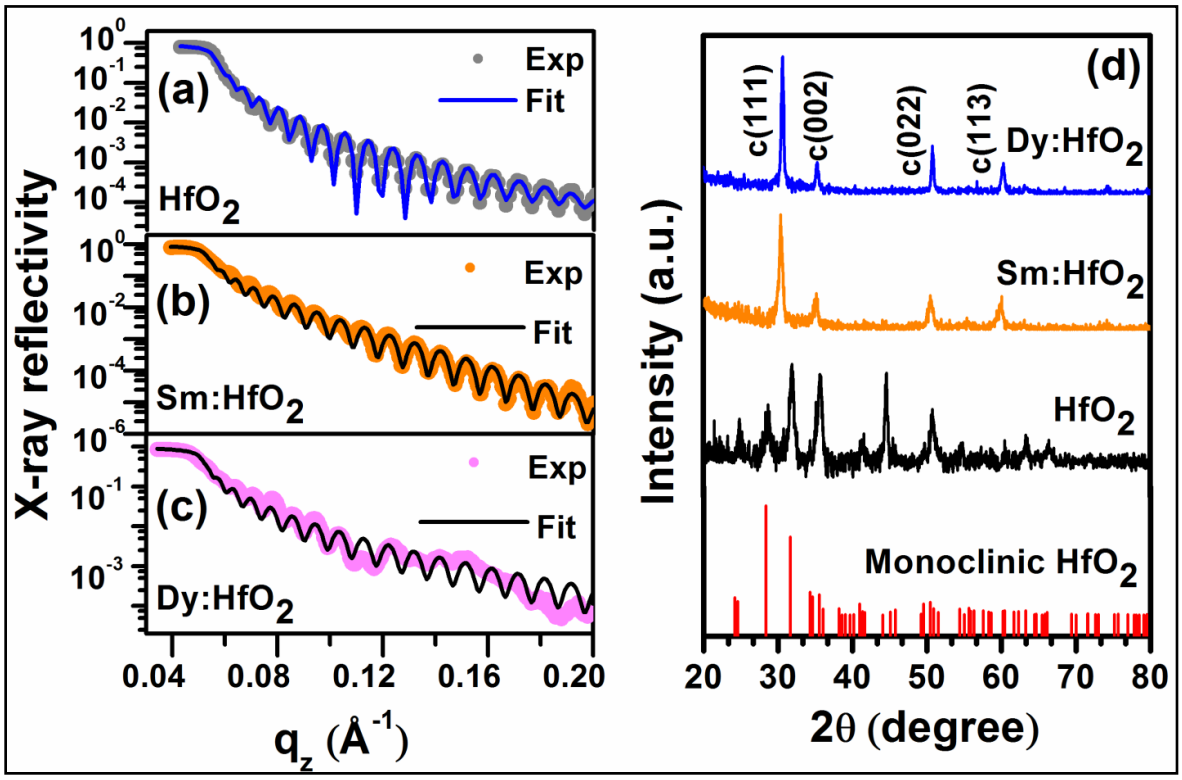

Figure 6.1 *X-ray reflectivity of* ***(a)*** *HfO_2,* ***(b)*** *Sm: HfO_2 and,* ***(c)*** *Dy:HfO_2;* ***(d)*** *GIXRD patterns of HfO_2, Sm:HfO_2 and Dy:HfO_2 films.*

The GIXRD patterns of HfO_2, Dy:HfO_2 and Sm:HfO_2 films annealed at 550 ^{0}C are depicted in **figure 1 (d)**. The presence of sharp diffraction peaks specify the crystalline nature of the films.For HfO_2, the diffraction peaks identified as (110), ($\bar{1}$11), (111), (020), (200), (021), ($\bar{2}$11) and(112) are well matched with the monoclinic phase of HfO_2, space group, $P2_1/c$ (JCPDS card no. 78-0049). However, after incorporating Sm or Dy, the observed peaks such as (111), (002), (022) and (113) are attributed to cubic phase of HfO_2,

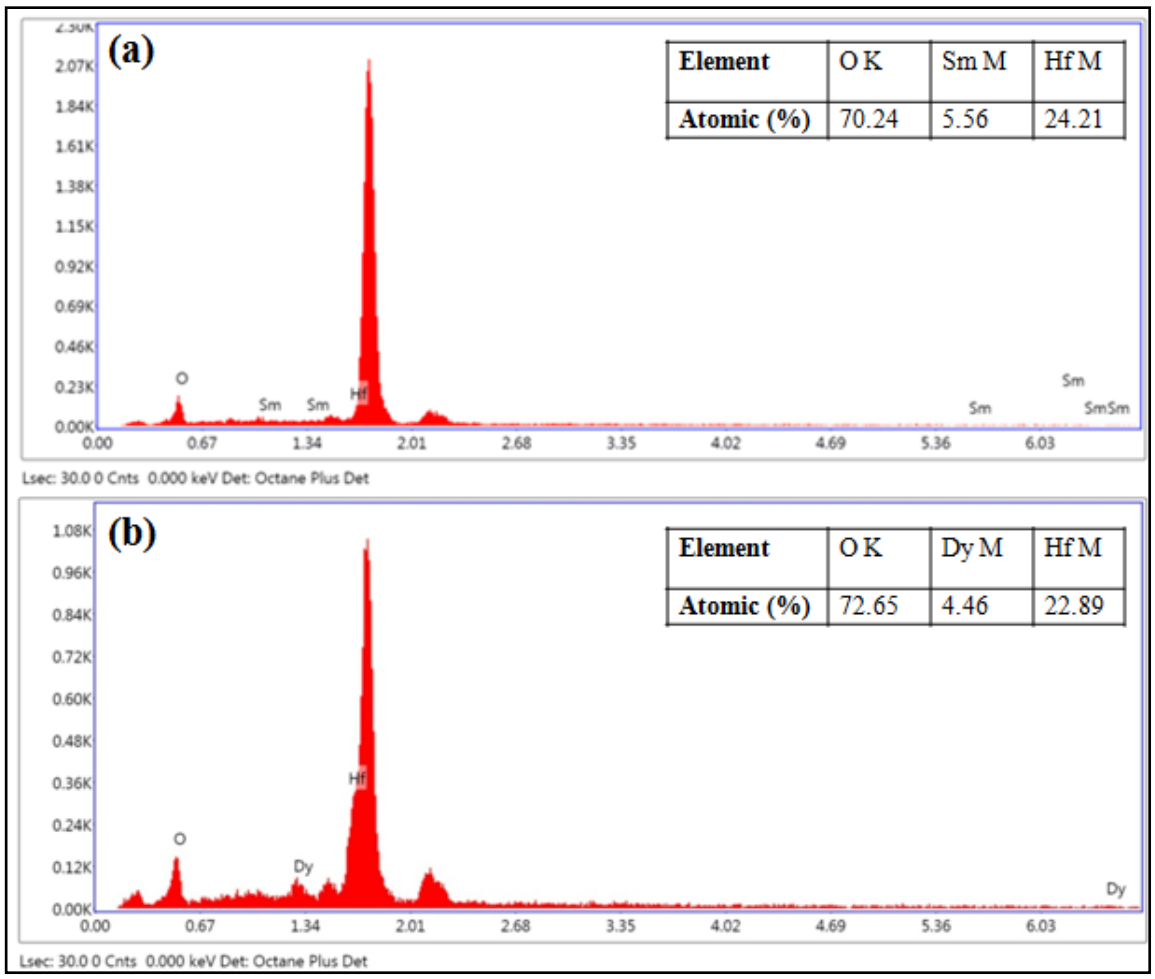

Figure 6.2 *EDS spectra for* ***(a)****Sm:HfO_2 and* ***(b)*** *Dy:HfO_2 films annealed at 550 ^{0}C.*

space group, $Fm\bar{3}m$ (JCPDS card no. 53-0560). Absence of secondary phase indicates that Dy^{3+} and Sm^{3+} ions substitute at Hf^{4+} site of HfO_2 lattice. Surprisingly, in Sm/Dy doped HfO_2 films, the high temperature cubic phase is stabilized at room temperature. Earlier, we have reported the stabilization of cubic phase at RT by incorporating 12 at% of Sm or 11 at% of Dy in HfO_2 nanoparticles. Here, the cubic phase is stabilized at most half concentration of these dopants in HfO_2 films compared to nanoparticles. In particular, the monoclinic to cubic phase transformation is explained considering the difference in ionic radii and oxidation states of Dy^{3+}, Sm^{3+} and Hf^{4+} ions resulting in formation of oxygen

vacancies.[189] It is well-known that the coordination numbers of Hf^{4+} ion in the monoclinic and cubic phase are 7 and 8, respectively.[66] When Sm^{3+} or Dy^{3+} replace Hf^{4+} ion, the oxygen vacancies are produced near dopant sites in HfO_2 lattice resulting in 8-fold oxygen coordination to dopant ions thereby stabilizing the cubic phase of HfO_2 at room temperature.

6.2.2 X-ray Photoelectron Spectroscopy

Therefore, we study the role of oxygen vacancy concentration in the stabilization of cubic phase of HfO_2 by means of XPS technique. **Figure 6.3 (a-c)** show XPS spectra of Hf 4*f* core levels for HfO_2, Dy:HfO_2 and Sm:HfO_2 films. The spectra are first corrected with respect to the C 1*s* peak located at ~284.6 eV. Hf 4*f* spectra have been deconvoluted into two peaks fitted with mixed Gaussian and Lorentzian functions using XPSPEAK version 4.1. The two peaks are found to be located at ~16.2 and ~17.9 eV associated to Hf $4f_{7/2}$ and Hf $4f_{5/2}$, respectively.[105] XPS spectra of O 1*s* are demonstrated in **figure 6.3 (a'-c')**. Due to asymmetric shape of the spectra, we have deconvoluted the spectra into two peaks named as Peak 1 and 2 found to be centered at ~530 and ~531 eV, respectively. In low binding energy (B.E) region, the peak at ~530 eV is ascribed to lattice oxygen atoms in Hf-O bonds whereas the high B.E peak at ~531 eV is attributed to oxygen deficient regions exhibiting oxygen vacancies and O_2^- ions in Si-O bonds.[66, 190] The area ratio under peak 2 and 1 i.e. (A_2/A_1) is found to be 0.60, 0.87 and 0.93 in HfO_2, Sm:HfO_2 and Dy:HfO_2 films, respectively. Although the oxygen vacancies exist in monoclinic phase HfO_2film, the notable increase in A_2/A_1 for Sm and Dy doped HfO_2 films thereby induce more and more oxygen vacancies in HfO_2 lattice. Thus, it is confirmed that an appropriate concentration of

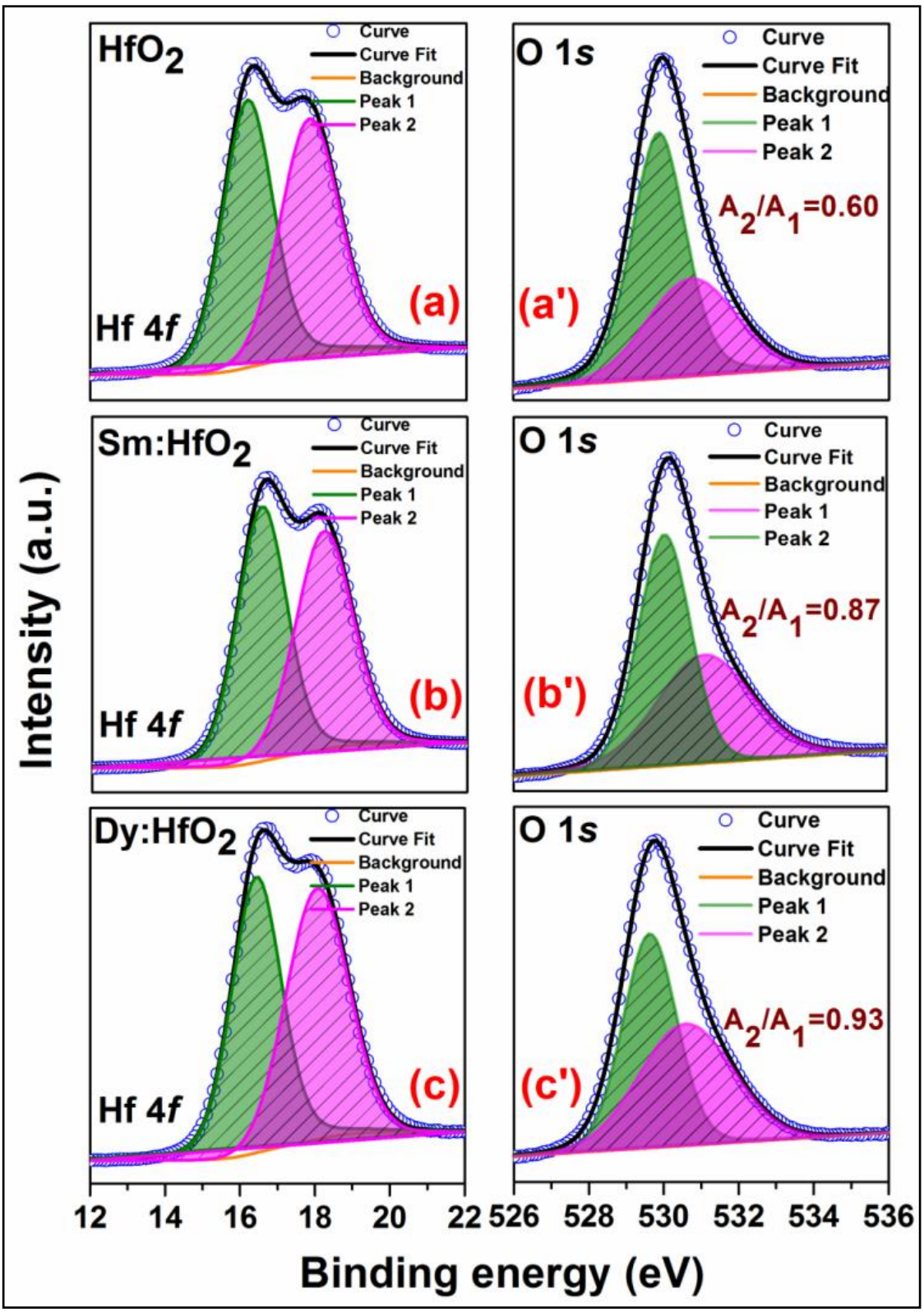

Figure 6.3 *The XPS spectra of Hf 4f and O1s core levels for* ***(a,a')*** *HfO_2,* ***(b,b')*** *Sm:HfO_2 and* ***(c,c')*** *Dy:HfO_2, respectively.*

oxygen vacancies are present in the host lattice which facilitate the stabilization of cubic phase in Sm and Dy doped HfO_2 film. Owing to abundance of oxygen vacancy, these films are explored for RRAM device application.

6.2.3 Current-Voltage (*I-V*) Characteristics

We investigate the resistive switching behavior of HfO_2 based RRAM using the semi-logarithmic current-voltage (*I-V*) characteristic curves for HfO_2, Sm:HfO_2 and Dy:HfO_2 thin film devices shown in **figure 6.4**. *I-V* measurements are performed after sweeping the applied DC bias voltage in a sequence of 0 V→ 4 V→ 0 V→ -5 V→ 0 V. During *I-V* measurements, the bottom electrode was grounded and the bias voltage applied to the top electrode. To avoid electrical breakdown of devices, the compliance current was fixed at 7 mA during switching measurements. At first stage (0→4 V), initially the value of current is very small indicating HRS or OFF-state and at a certain bias voltage known as SET voltage (V_{SET}), the current shows an abrupt enhancement indicating switching towards LRS or ON-state. Similarly, in negative bias voltage region (0→-5 V), the bias voltage at which the current decreases sharply is called as RESET voltage (V_{RESET}). The existence of positive V_{SET} and negative V_{RESET} confirms the distinct bipolar resistive switching behavior in our HfO_2 based RRAM devices. Interestingly, the resistive switching characteristic is of forming-free nature. V_{SET} value is found to be ~3.7 V for monoclinic phase HfO_2 device whereas the cubic phase Sm:HfO_2 and Dy:HfO_2 RRAM exhibit ~3.2 and 2.8 V, respectively. Also, the separation between ON and OFF states estimated as approximately three is feasible for RRAM device.

To understand and obtain a detailed insight into SET and RESET mechanisms, we investigate different conduction models such as Schottky emission, Poole-Frenkel (P-F)

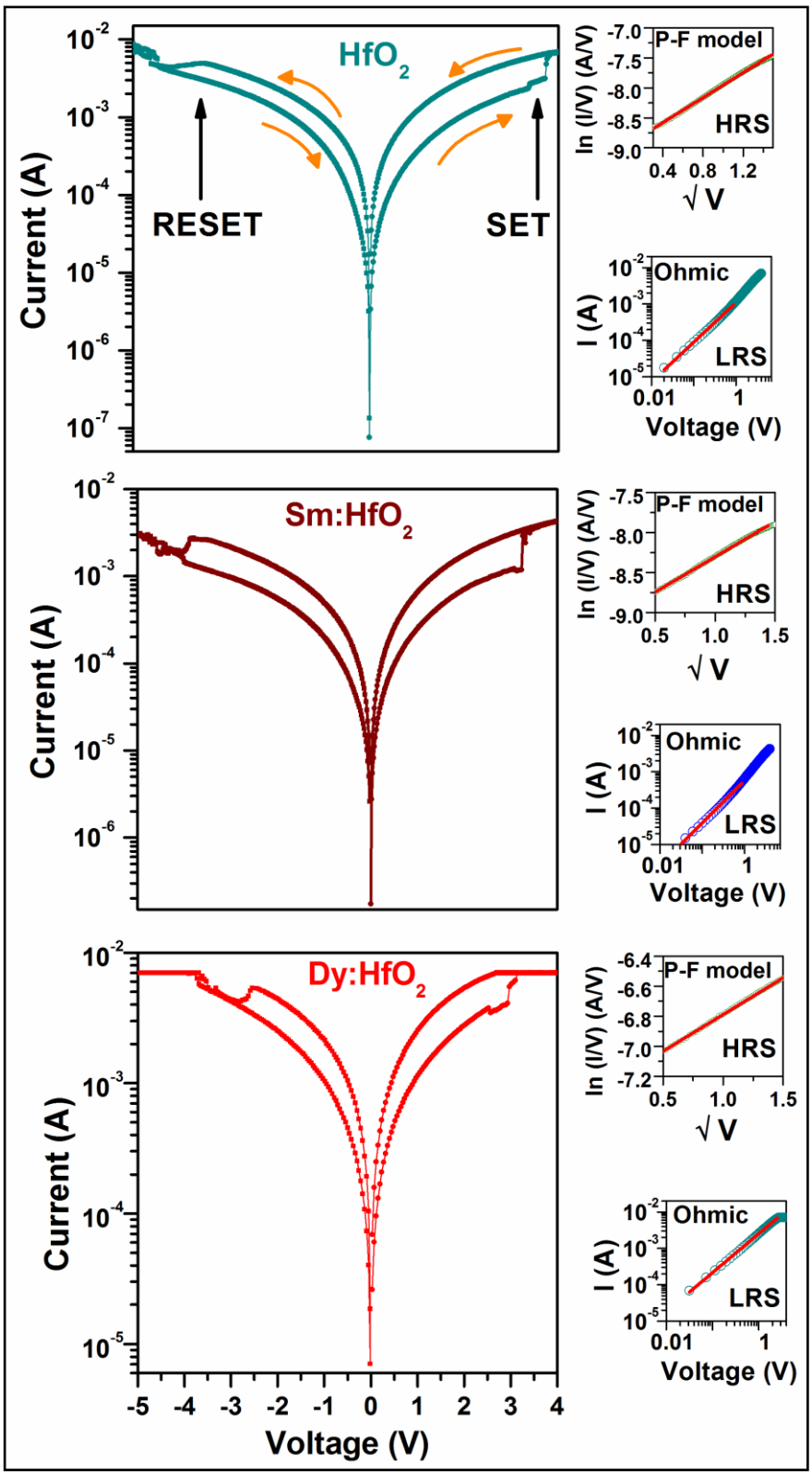

Figure 6.4 *Current-Voltage (I-V) characteristics in semi-logarithmic scale for HfO_2, Sm:HfO_2 and Dy:HfO_2.thin film devices. Insets show P-F and Ohmic model linear fits for HRS and LRS resistive states, respectively.*

emission, Ohmic conduction and Fowler-Nordheim (F-N) tunneling and space charge limited current (SCLC) in LRS and HRS states.[97] The current and voltage relationships for Ohmic conduction and P-F emission are given as $I= Ve^{-A/T}$ and $I=Ve^{\frac{q}{kT}(2a\sqrt{V-\phi_B})}$, respectively, where *A*is a constant, T is temperature, $a=\sqrt{q/4\pi\varepsilon_i d}$, ε_i is electric field in dielectric, d is the thickness of dielectric, ϕ_B is barrier height and k is called as the Boltzmann constant.[191] The right panel of **figure 6.4**, for HfO_2 based RRAM, depicts fitting of *I-V* behavior in log-log scale confirming a linear relationship having slope of 1-1.2. This indicates that the Ohmic conduction is dominant in complete LRS state, however, the conduction behavior within low voltage regime for HRS state also follows only the Ohmic model. Ohmic conduction prevails when the thermally generated carrier density is sufficiently higher than that of the injected carrier density. Nevertheless, in case of high voltage regime of HRS, the conduction mechanism is somewhat different and does not follow a linear behavior. Such behavior can be perceived by applying the nonlinear conduction mechanism like P-F emission. The right panel of **figure 6.4** provides linear fits of *I-V* curves to P-F emission model in the high applied bias voltage region of HRS state. It is confirmed that P-F emission is the key conduction mechanism in high electric field range. P-F emission conduction occurs essentially due to the crystalline defects in HfO_2 films like single (V_o^+) or doubly (V_o^{++}) charged oxygen vacancies. This conduction mechanism is related to the trap assisted tunneling process inducing lowering of the voltage barrier which is a manifestation of the Coulomb attraction between the positively charged traps and negatively charged conduction electron into the conduction band.[192] Similar conduction mechanisms of Ohmic and P-F emission govern LRS and HRS in case of Sm and Dy:HfO_2 devices.

Further, the resistive switching behavior in RRAMs has been explained in terms of the formation of conductive filaments (CFs), migration of oxygen vacancies/ions, Schottky barrier and trapped charged carriers.[98] Among them, the resistive switching behavior in HfO_2 based RRAM is being widely studied considering the localized formation and rupture of CFs within the dielectric film. It is known that under small bias voltage, localized nanosize CFs are formed in oxide film which segregate to produce the stronger and more conductive CFs at higher applied bias voltage. These CFs are mainly comprised of charged oxygen vacancies generating conduction electrons.[98] In this context, Zhang *et al*. investigate that Gd doping in HfO_2 lattice enhances RRAM behavior by minimizing the randomized nature of CFs thereby reducing oxygen ion migration barrier.[104] Lee *et al*. demonstrate that while Gd and Dy doped ZrO_2 devices exhibit switching behavior due to sufficiently large concentration of dopant induced oxygen vacancies, Ce doped ZrO_2 based RRAM shows initial formation of CF which is ascribed to improved crystallization/densification.[193] On the other hand, in $Gd_2O_3$and HfO_2based RRAM, a similar role of abundant defects such as oxygen vacancies rendering forming-free switching behavior have been reported.[194, 195] In the present case, in pristine and Sm or Dy doped HfO_2 films, the presence of sufficiently high concentration of oxygen vacancies not only shows the monoclinic to cubic phase transformation at RT but also contribute towards resistive switching behavior which is of forming-free nature as reported by others.

A schematic illustration of possible resistive switching mechanism through formation of CFs for HfO_2 based RRAMs is depicted in **figure 6.5**. Without bias, the oxygen vacancies present in the film move with random motion. After applying the bias voltage, the current increases considerably indicating partial formation of CFs.

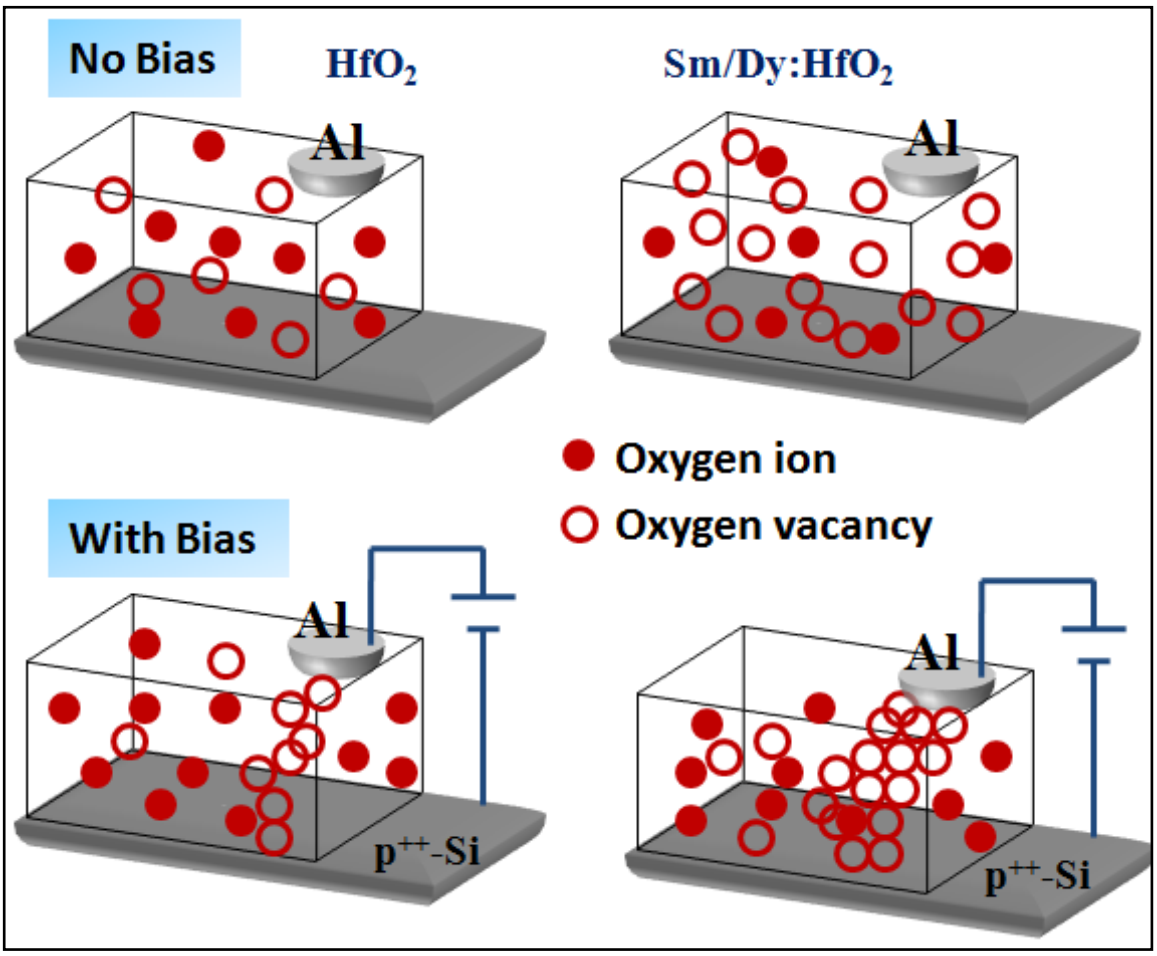

Figure 6.5 *The proposed schematic diagram illustrating resistive switching mechanism through CFs formation in pristine and Sm or Dy doped HfO_2 RRAM devices.*

At a certain V_{SET} value, all the localized CFs redistribute and combine to form a highly conducting filament containing a more oriented segregation of V_O leading to switching of HRS to LRS state. On the other hand, for negative applied DC voltage, these CFs dissolve and eventually rupture because of the Joule heating effect resulting in LRS to HRS switching at V_{RESET} voltage.[101] In case of Sm or Dy doped HfO_2 devices, the concentration of V_o is relatively higher due to substitution of Dy^{3+} or Sm^{3+} ion atHf^{4+} site generating more number of V_O in the lattice evidenced from XPS analysis. The

incorporation of Dy^{3+} or Sm^{3+} ion in HfO_2 reduces the formation energy required to form V_o by creating dipoles between V_o and dopants. As a consequence, V_o tends to reside near dopant site in HfO_2 lattice providing improved control of CFs formation.[104] This could allow a well controlled resistive switching from HRS to LRS at a lower V_{SET} value in Sm or Dy doped HfO_2 based RRAM devices. These devices would be promising for application in next generation data storage.

6.3 Conclusions

To summarize, pristine and Sm, Dy doped HfO_2 films were deposited on p^{++}-Si (100) substrates having film thickness of ~60 nm with an appropriate film density of ~9.2-8.1 g/cm^3. We observed that while pristine film exhibited the monoclinic phase, the high temperature cubic phase was stabilized at RT in Sm or Dy doped HfO_2 film after doping at most half concentration of these dopants compared to nanoparticles. The monoclinic to cubic phase transformation was attributed to formation of oxygen vacancies understood from XPS analysis. Due to the presence of oxygen vacancies, we carried out the bipolar resistive switching behavior for RRAM device application. The ON/OFF separation was estimated to approximately three and the resistive switching characteristics was of forming-free nature feasible for RRAM device. After fitting appropriate conduction models, it was confirmed that the Ohmic and P-F emission conduction mechanisms dominated in LRS and HRS states, respectively. The switching behavior was ascribed to the formation and rupture of conducting filaments comprised of oxygen vacancies under positive and negative applied bias, respectively. Therefore, an abundance of oxygen vacancies forming 8-fold oxygen coordination to dopant ion played a crucial role in the stabilization of cubic phase

at RT and also governed the forming-free switching behavior inHfO_2 based RRAM devices.

Chapter 7

This thesis provided a comprehensive investigation on the structure, magnetic, optical and electrical properties of multifunctional nanostructured pure, Dy and/or Sm doped HfO_2. The present work dealt with two different forms i.e. nanoparticles and thin films of HfO_2. The high temperature tetragonal and cubic phases of HfO_2 are promising from industrial point of view due to their appropriate high-*k* value which facilitate the fabrication of CMOS devices with improved performance. In this context, we particularly examined the stabilization of cubic phase at room temperature after incorporating Dy and/or Sm into HfO_2 lattice. In addition to intriguing structural transformation, the systematic studies on the effect of Dy and/or Sm dopants in modifying magnetic, optical and electrical properties produced captivating results which could be implemented for practical applications like LFPs imaging for the first time and as non-volatile data storage in RRAM devices. The key findings of the thesis are outlined below.

7.1 Stabilization of the High Temperature Cubic Phase at Room Temperature

HfO_2 nanoparticles synthesized via a Pechini type sol–gel technique crystallized with monoclinic phase, $P2_1/c$, at room temperature. By incorporating 11 at% of Dy into the HfO_2 lattice, the monoclinic phase transformed completely to the cubic phase, $Fm\bar{3}m$, followed by a mixed phase of monoclinic and cubic at intermediate concentrations (5–9 at%) of Dy. In case of Sm doped HfO_2, although the monoclinic structure was retained at 1 at% of Sm, the monoclinic to cubic phase transformation at room temperature was achieved by incorporating Sm^{3+} ions upto 12 at% followed by the coexistence of